PHYSICAL REVIEW B **81**, 161410(R) (2010)

Selective formation of ABC-stacked graphene layers on SiC(0001)

Wataru Norimatsu and Michiko Kusunoki
EcoTopia Science Institute, Nagoya University, Furo-cho, Chikusa-ku, Nagoya-shi, Aichi-ken 464-8603, Japan
and Materials Research and Development Laboratory, Japan Fine Ceramics Center, 2-4-1, Mutsuno, Atsuta-ku, Nagoya-shi, Aichi-ken 456-8587, Japan

(Received 23 February 2010; published 21 April 2010)

An investigation using high-resolution transmission electron microscopy of the stacking sequence of several layers of graphene formed on SiC(0001) shows that graphene layers selectively exhibit an ABC-type stacking. Using the well-known Slonczewski-Weiss-McClure model based on the tight-binding method, we suggest that a γ_5-like interatomic interaction, which corresponds to the formation of a linear trimer of ABA type stacking, is spontaneously weakened by the interaction between graphene and SiC. This can lead to the destabilization of the ABA stacking and to the formation of the ABC stacking, indicating the possibility of bandgap tuning by an electric field in more than three layers of graphene on SiC.

DOI: 10.1103/PhysRevB.81.161410 PACS number(s): 61.48.De, 68.37.Og, 73.20.At, 81.05.U−

Graphene has an extremely high electronic mobility, in addition to anomalous electronic properties as a two-dimensional material, which raises hopes for its use as a next-generational semiconducting material.[1–4] The electronic states of several layers of graphene vary drastically depending on the number of layers and the stacking sequence.[5–7] As for the stacking sequence of bulk graphite, it is known that there are three types: an AA stacking (simple hexagonal, space group of $P6/mmm$), an AB stacking (hexagonal, called Bernal, $P6_3/mmc$), and an ABC stacking (rhombohedral, $R\bar{3}m$).[8,9] Figures 1(a)–1(c) show the crystal structures corresponding to these stackings. A random stacking of these three types is called a turbostratic (TS) structure. An ambipolar transport has been demonstrated experimentally in the Bernal stacking while an electric-field-induced band-gap opening was predicted in the AB-bilayer, ABC-trilayer, and ABCA-tetralayer stackings.[5–7] Thus, both determination and control of the stacking sequence are necessary for graphene-based electronics. In bulk graphite, it was reported that the volume fraction AB:ABC:TS was about 80:14:6, and the total energy difference between AA and AB was 17.31 meV/atom, and between ABC and AB was 0.11 meV/atom.[8,9] These tiny energy differences indicate the difficulty of inducing selective formation of AB and ABC stackings. On the other hand, in the isolated bilayer graphene, an AA stacking was frequently observed, according to a recent report.[10]

One of the production processes for well-controlled graphene layers is the SiC surface decomposition method.[11–17] In this method, silicon atoms are sublimed from the SiC surface by high-temperature annealing in a vacuum furnace and the remaining carbon atoms form graphene layers. Graphene layers formed on SiC have some advantages, such as their spontaneous formation on the insulating substrate, the possibility of wafer-scale production, and potential controllability of electronic states by exploiting the interaction between the graphene and SiC.[13,14] A few previous studies assumed coexisting of the ABA and ABC stacking to explain the results of photoemission spectroscopy and scanning tunneling spectroscopy measurements.[18–20] In other words, the stacking sequence of graphene on SiC has not yet been directly elucidated. In this Rapid Communication, we show that the ABC-stacked graphene uniquely appears on the SiC(0001) substrate. We discuss the selective formation of the ABC stacking with respect to the structural stability using a density-functional calculation and the tight-binding method.

The sample preparation procedure for graphene on Si-terminated SiC was described in our previous paper.[16] Commercially available on-axis 6H-, on-axis 4H-, and 4° off-axis 4H-SiC substrates were used. Using our vacuum furnace, Si sublimation leads to the carbon nanocap formation at lower temperature than 1300 °C,[11] in contrast to the small-area and low-quality graphene formation at higher temperatures than 1350 °C due to going through the process of nanocap formation at lower temperatures. To prepare large-area and high-quality graphene, the surface of the SiC substrates was oxidized at 1200 °C in O_2 atmosphere. The oxidized layer on the surface remains up to 1300 °C even in vacuum but sublimes above that temperature and prevent nanocap formation, resulting in large-area and atomically flat graphene growth with more than several micrometers width. The image of the obtained large-area graphene is shown in Fig. 2(a). Graphitization temperatures were 1350–1450 °C. Thin specimens for high-resolution transmission electron microscope (HRTEM) observations were prepared by Ar-ion thinning. The observations were carried out in a JEM-2010F TEM. The stacking sequence of graphene layers was analyzed by a fast Fourier transformation (FFT) treatment of the observed images. In order to investigate the structural stability energetically, first-principles calculations based on density-functional theory (DFT) were performed using the ABINIT code.[21,22] Pseudopotentials for the generalized gradient approximation (GGA), 707 eV cut-off energy, $8\times8\times1$ Brillouin zone integration, and a 2-nm-thick vacuum layer were used for the calculations. As for the atomic structure, the $(2\times2)_{\text{graphene}}$-on-$(\sqrt{3}\times\sqrt{3}R30)_{\text{SiC}}$ supercell, the interface structure which we clarified previously,[16] and lattice constants and interlayer distances of the bulk graphite crystal were used. In addition, the values of the tight-binding parameters in the Slonczewski-Weiss-McClure (SWMcC) model[23–26] enabled a qualitative discussion of the selective formation of ABC-stacked graphene.

Before proceeding to the experimental results, we first

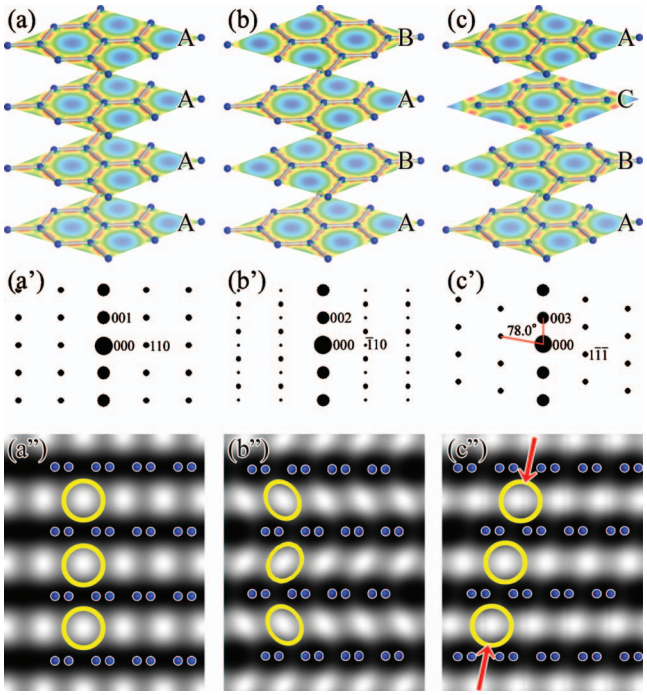

FIG. 1. (Color) Structures of (a) AA-, (b) AB-, and (c) ABC-stacked graphene layers. Simulated $[11\bar{2}0]_{\text{graphite}}$ electron diffraction patterns of (a′) AA-, (b′) AB-, and (c′) ABC stackings. Diffraction spots are indexed in (a′) $P6/mmm$, (b′) $P6_3/mmc$, and (c′) $R\bar{3}m$ notations. Simulated HRTEM images of (a″) AA-, (b″) AB-, and (c″) ABC-stacked graphite. The simulation was carried out for a 40 nm underfocus and a sample thickness of 3 nm. Blue balls represent carbon atoms and yellow circles are guides to the eye to clarify the stacking sequence.

comment on the crystallographic features of graphene on SiC. The unit cell of graphene is known to be rotated by 30° with respect to that of the SiC. This means that the orientation relationship between graphene and Si-terminated SiC is $[1\bar{1}00]_{\text{SiC}} \| [11\bar{2}0]_{\text{graphene}}$. Figures 1(a′)–1(c′) show simulated $[11\bar{2}0]$ electron diffraction patterns of AA-, AB-, and ABC-stacked graphite, respectively. These diffraction patterns are clearly different from one another. In particular, the extinction rules for the $11l$, $\bar{1}1l$, and $1\bar{1}l$ systematic reflections for, respectively, AA-, AB-, and ABC-stacking differ. Among them, the ABC stacking is characterized by the angle of 78.0° between the 003 and $\bar{1}11$ reflections. That is, we can distinguish the stacking sequence of graphene with HRTEM along the $[11\bar{2}0]_{\text{graphene}}$ direction, which corresponds to the $[1\bar{1}00]$ direction of the SiC substrate. In Figs. 1(a″)–1(c″), simulated HRTEM images of AA-, AB-, and ABC-stacked graphite are shown, with the atom positions shown as blue circles. One of the characteristic features is the presence of a bright dotted contrast between graphene layers. In the AA stacking, bright dots are arranged in lines perpendicular to the graphene plane, in the AB stacking, dots exhibit a zigzag pattern, and in the ABC stacking, dots are arranged linearly, but are not perpendicular to the plane.

Figure 2 shows HRTEM images of graphene layers formed on (b) 4H-SiC and (c) 6H-SiC. The observation condition is about a 40 nm underfocus. Under this condition, the atom positions are observed as a dark contrast, which was carefully checked by the image simulation. Several layers of graphene on SiC substrates are seen as a dark line contrast in both samples. And as the characteristic feature, we can confirm that the bright dotted contrast between graphene layers in Fig. 2 occur on a linear slant, suggesting the ABC stacking. This feature can be observed in the whole terrace region such as shown in Fig. 2(a).

In order to confirm this interpretation, we performed FFT treatments of the HRTEM images. The FFT pattern of an HRTEM image is generally equivalent to the electron diffraction pattern. Figures 2(b′) and 2(c′) show the FFT patterns of the corresponding HRTEM images. In both patterns, there are sequences of diffraction spots indicated by the blue and red arrows. We analyzed these diffraction spots and concluded that the blue-arrowed spots could be explained as the Bragg reflections in the $[1\bar{1}00]_{\text{SiC}}$ electron-diffraction pattern while those indicated by the red arrows are due to the graphene layers. The extinction rule and the interplanar angles of 78.2 and 78.5° well coincide with those in Fig. 1(c′), indicating the ABC stacking. The diffuse streaks along the c^* axis also found in both (b′) and (c′) can be understood as a result of the shape effect due to the presence of the interface and the surface. It should be noted here that our results obtained from graphene layers on both 4H- and 6H-SiC substrates were almost the same. This means that a different stacking sequence in SiC does not affect the stacking of graphene layers on the surface.

We here discuss the selective formation of the ABC stacking. First, we performed a DFT calculation in order to evaluate the energetic differences in the stability of different stack orderings. We calculated the total energies of ABAB- and ABCA-tetralayer graphene on SiC. The obtained total energies were −7365.3234 and −7365.3240 eV for ABAB and ABCA stackings, respectively. The difference between these two results is only 0.000008%, which is clearly within the computational error. Thus, pursuing an energetic investigation to distinguish between ABA and ABC stacking was not practical using DFT calculations. This may be because the GGA is not good at dealing with the van der Waals interaction between the graphite layers. In other words, the interlayer interaction should be treated directly in order to probe the selectivity of stack orderings.

We introduce the well-known SWMcC model to consider the stacking sequence in terms of interatomic interactions, including those between layers.[23–26] In the SWMcC model, the characteristic features of the electronic states in AB-stacked graphite are described by the γ_0-γ_6 interatomic interactions, which is based on a tight-binding framework. This suggests that these γ_n-like interatomic interactions are involved in to the structural stability of bulk graphite, where the AB stacking is slightly stable compared with the ABC stacking. Among these interactions, the γ_0 interaction between in-plane adjacent atoms, the γ_1, γ_3, and γ_4 ones between atoms of neighboring layers, and the chemical shift γ_6 between two atoms in the unit cell are all clearly equivalent for ABA and ABC stackings. On the other hand, the γ_2- and γ_5-interatomic interactions of the next-neighboring layers are

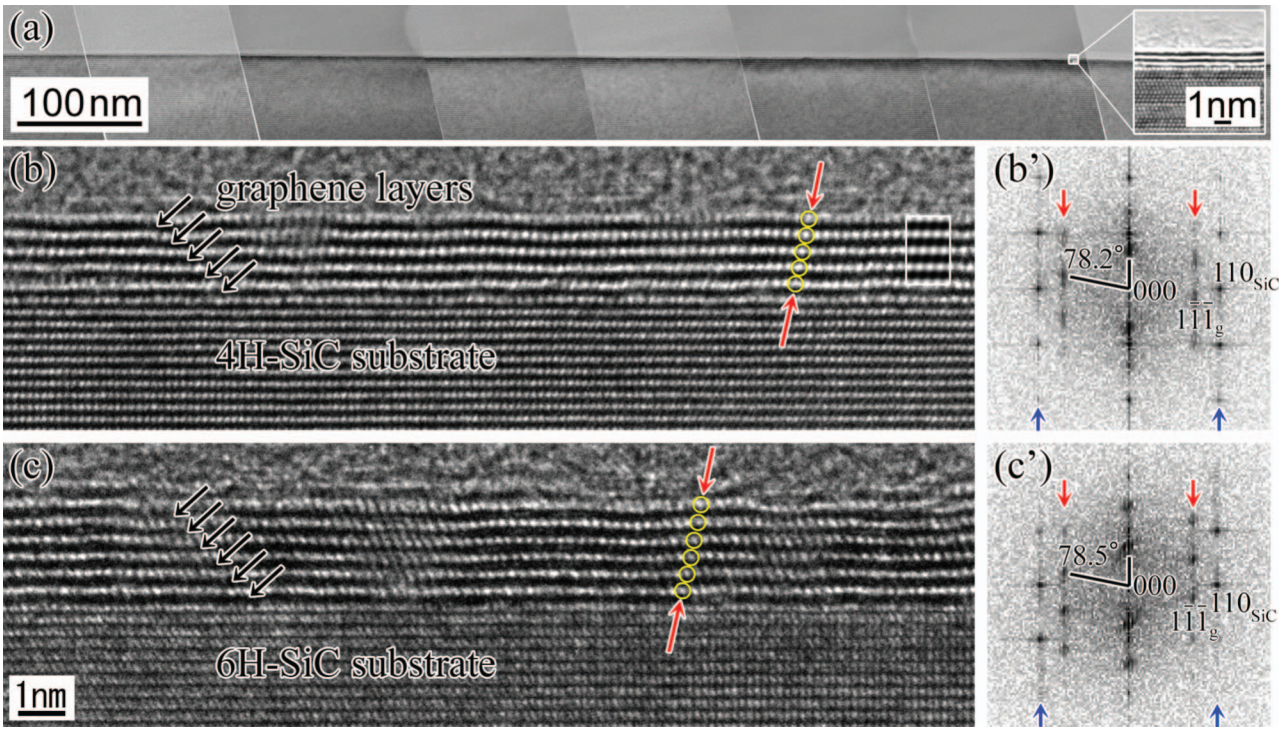

FIG. 2. (Color) TEM images of graphene layers on [(a) and (c)] 6H- and (b) 4H-SiC. In the low magnification image together with the inserted high magnification image in (a), the electron beam is incident parallel to the $[11\bar{2}0]_{SiC}$ direction, while in (b) and (c), it is parallel to the $[1\bar{1}00]_{SiC}$ direction. Graphene layers are observed as the dark lines indicated by the black arrows. A simulated HRTEM image of ABC stacking is shown in the inset in (b). In (b′) and (c′), FFT patterns of the area around (b) and (c) are shown. Diffraction spots along the red arrow directions correspond to those in the image in Fig. 1(c′), indicating ABC stacking.

different for the two stackings. Figures 3(a) and 3(b) show these two interactions in the ABA and ABC stackings. Both ABA and ABC stackings have a γ_2 interaction, but in the ABC-stacked layers, there is no γ_5 interaction, corresponding to the formation of a linear trimer in the ABA stacking. This suggests that the presence of the γ_5-like interatomic interaction is a major contributor to the stability of ABA stacking relative to ABC stacking in bulk graphite.

We can further apply the argument above to the stack ordering of graphene layers on SiC. It has been accepted that there is a strong covalent bond between some of the carbon atoms in first carbon layer and some of the silicon atoms on the top of the SiC substrate.[13,15,16] In the interface of $(2\times2)_{graphene}$-on-$(\sqrt{3}\times\sqrt{3}R30)_{SiC}$ supercell, there are three Si atoms, eight C atoms, and two covalent bonds among them. This covalent bond causes a displacement of the carbon atom toward the silicon atom below. The displacement breaks the symmetry in the first carbon layer, resulting in the anomalous electronic properties of graphene on SiC. According to our previous study, the carbon atoms in the first carbon layer displace vertically by 0.3 Å downward, as shown in layer A of Fig. 3(b).[16] Here, we assume the ABA-stacked graphene on SiC; that is, the third carbon layer is the A layer. In this case, we can easily suppose that the above-mentioned atomic displacement weakens the γ_5-like interatomic inter-

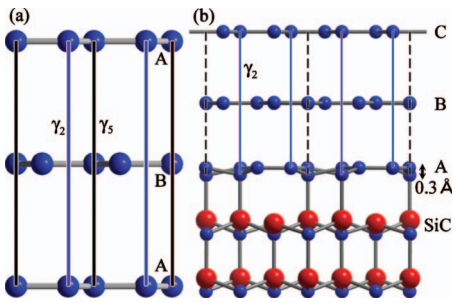

FIG. 3. (Color) Schematic model of the meaning of the SWMcC γ parameters in (a) AB stacking and (b) the structure of ABC-stacked graphene on SiC from the $[1\bar{1}00]_{SiC}$ direction. The γ_2 and γ_5 interactions are indicated by the blue and the black lines in (a).

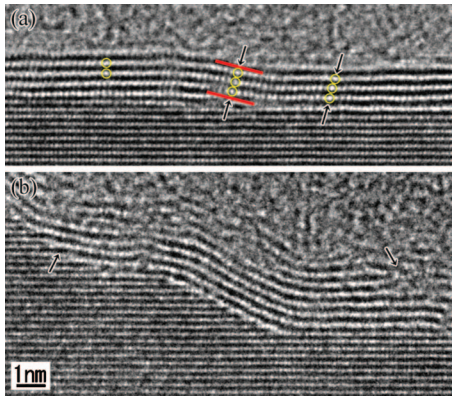

FIG. 4. (Color) HRTEM images of graphene layers formed on SiC around a step. Arrows and circles are guides to the eye.

action due to the increased distance between the carbon atoms in the first A layer and the third A layer in Fig. 3(a).

Thus, the spontaneously weakened γ_5-like interaction due to the presence of the SiC substrate may affect the stability of the stack ordering and the total-energy difference between the ABA and ABC stacking may be reversed. It is then suggested that the relatively stable ABC stacking can appear due to the destabilization of the γ_5-like interaction which characterizes the AB stacking. In other words, after the formation of two layers of graphene with AB stacking on SiC, a C layer may selectively form as the third layer.

The interaction between graphene and SiC also has an influence on the γ_2 interaction denoted by the black arrows in Fig. 3. However, the γ_2 interaction is equivalent for both ABA and ABC stacking, and hence does not contribute to the difference of stability. In fact, there is a higher-order β_5 interaction in the ABC stacking instead of a γ_5 one.[27] It was also reported that the β_5 interaction in ABC stacking is markedly smaller than the γ_5 one in AB stacking. We can then ignore the β_5-like interaction as an approximation. From the qualitative discussion above, we propose that the ABC-stacked graphene layers on SiC are stabilized because of the reduced γ_5-like interaction.

We also examined the stacking sequence of graphene layers in the vicinity of a SiC step. Figure 4 shows the HRTEM images of graphene around a step present on the off-axis 4H-SiC substrate. In Fig. 4(a), graphene layers exist that cover the step to a height of two SiC bilayers. In the terrace region, the stacking sequence is ABC type, as shown by the right arrows. As a result of continuous formation of graphene from the right, bright dots arrange in a line perpendicular to the slope as indicated by red lines. This indicates the presence of AA- or AB-type stacking sequence in this local region in (a). In another region having steeper slope, such as that in Fig. 4(b), clear bright dots are not visible, suggesting the turbostratic structure. We then conclude that around a step, the stacking sequence becomes disordered, in contrast to the terrace regions. In addition, in the vicinity of the steep step as in Fig. 4(b), graphene layers have a tendency to be discontinuous. It should be emphasized that the ABC stacking feature was observed everywhere in the terrace regions.

Recently, a report of electric-field-induced band-overlap tuning observed experimentally in trilayer graphene has appeared.[28] A previous study reported theoretically that the magnitude of the band gap can be controlled by an electric field in ABC-stacked trilayer graphene and in ABCA-stacked tetralayer graphene.[6] Our present observation revealed that the ABC-stacking was stabilized in graphene having more than three layers formed on SiC; nevertheless in bulk graphite, AB stacking is the most stable. Therefore, it is possible that a gap-tunable semiconductor controlled by an electric field can be fabricated using graphene layers obtained by the SiC flat-surface decomposition method.

In conclusion, we have clarified by HRTEM observations that the stack ordering of graphene layers formed on SiC(0001) is of the ABC type. Selective formation of the ABC stacking can be explained by spontaneous weakening of the γ_5-like interaction due to the interaction between the graphene and the substrate. This weakening destabilizes the linear trimer of the ABA stacking and results in the formation of the next most stable ABC stacking. Our finding may play an important role in clarifying the path to the creation of a tunable gap semiconductor made from graphene having more than three layers.

This work was partially supported by the Asahi Glass Foundation.

[1] K. S. Novoselov *et al.*, Science **306**, 666 (2004).
[2] K. S. Novoselov *et al.*, Nature (London) **438**, 197 (2005).
[3] S. V. Morozov *et al.*, Phys. Rev. Lett. **100**, 016602 (2008).
[4] X. Hong *et al.*, Phys. Rev. Lett. **102**, 136808 (2009).
[5] S. Latil *et al.*, Phys. Rev. Lett. **97**, 036803 (2006).
[6] M. Aoki *et al.*, Solid State Commun. **142**, 123 (2007).
[7] Y. Zhang *et al.*, Nature (London) **459**, 820 (2009).
[8] R. R. Haering, Can. J. Phys. **36**, 352 (1958).
[9] J.-C. Charlier *et al.*, Carbon **32**, 289 (1994).
[10] Z. Liu *et al.*, Phys. Rev. Lett. **102**, 015501 (2009).
[11] M. Kusunoki *et al.*, Appl. Phys. Lett. **77**, 531 (2000).
[12] C. Berger *et al.*, Science **312**, 1191 (2006).
[13] S. Y. Zhou *et al.*, Nat. Mater. **6**, 770 (2007).
[14] K. V. Emtsev *et al.*, Nat. Mater. **8**, 203 (2009).
[15] J. Hass *et al.*, J. Phys.: Condens. Matter **20**, 323202 (2008).
[16] W. Norimatsu *et al.*, Chem. Phys. Lett. **468**, 52 (2009).
[17] W. Norimatsu *et al.*, J. Nanosci. Nanotechnol. **10**, 3884 (2010).
[18] T. Ohta *et al.*, Phys. Rev. Lett. **98**, 206802 (2007).
[19] P. Lauffer *et al.*, Phys. Rev. B **77**, 155426 (2008).
[20] J. Hass *et al.*, Phys. Rev. Lett. **100**, 125504 (2008).
[21] X. Gonze *et al.*, Comput. Mater. Sci. **25**, 478 (2002).
[22] See http://www.abinit.org for the official developer website.
[23] J.-C. Charlier *et al.*, Phys. Rev. B **43**, 4579 (1991).
[24] D. Nguyen-Manh *et al.*, Bull. Mater. Sci. **26**, 27 (2003).
[25] J. C. Slonczewski *et al.*, Phys. Rev. **109**, 272 (1958).
[26] J. W. McClure, Phys. Rev. **108**, 612 (1957).
[27] C. L. Lu *et al.*, Eur. Phys. J. B **60**, 161 (2007).
[28] M. F. Craciun *et al.*, Nat. Nanotechnol. **4**, 383 (2009).